2024 6th International Conference on Electrical Engineering and Information & Communication Technology (ICEEICT)
02-04 May 2024, Military Institute of Science and Technology (MIST), Dhaka-1216, Bangladesh

2024 6th International Conference on Electrical Engineering and Information & Communication Technology (ICEEICT) | 979-8-3503-8577-9/24/$31.00 ©2024 IEEE | DOI: 10.1109/ICEEICT62016.2024.10534355

Wavelet-Aided OTFS for Optical Wireless Communication

Mahmudul Hasan Abid
ECE Discipline
Khulna University
Khulna-9208, Bangladesh
Email: msc230902@ku.ac.bd

Iffat Ara Talin
ECE Discipline
Khulna University
Khulna-9208, Bangladesh
Email: msc230903@ku.ac.bd

Mohammad Ismat Kadir
ECE Discipline
Khulna University
Khulna-9208, Bangladesh
Email: ismat.kadir@ece.ku.ac.bd

***Abstract*—Orthogonal time frequency space (OTFS), a cutting-edge modulation technique, has gained attention as a potential prospect for future wireless communication. This paper incorporates wavelet transform in the conventional OTFS modulation, thereby presenting a method termed wavelet-aided OTFS (W-OTFS) modulation. The W-OTFS is then applied to optical wireless communication. In particular, a DC-biased optical W-OTFS (DCO W-OTFS) system is conceived, offering reduced spectral loss and peak-to-average power ratio (PAPR) in comparison to existing approaches. The proposed scheme outperforms both direct current optical (DCO) and asymmetrically clipped optical (ACO) OTFS schemes in terms of the PAPR and spectral efficiency. Additionally, the DCO W-OTFS is found to exhibit a lower bit error rate (BER) than the conventional DCO-based schemes.**

***Index Terms*—Wavelets, orthogonal time frequency space (OTFS), DCO W-OTFS, visible light communication (VLC)**

I. Introduction

Over the past few years, optical wireless communication (OWC) has been recognized as a potential contender for next-generation networks. The tremendous increase in data traffic requires a huge network capacity. While current infrastructure primarily relies on the RF spectrum, its limited bandwidth cannot meet the demands of next-generation networks. On the other hand, OWC can exploit an underutilized bandwidth extending up to the terahertz (THz) range. Various RF modulation schemes, such as orthogonal frequency division multiplexing (OFDM) and orthogonal time frequency space (OTFS), have been explored for multicarrier OWC, termed as optical OFDM (O-OFDM) and optical OTFS (O-OTFS), respectively. [1], [2]. Especially, O-OFDM has been intensively explored.

In optical wireless systems, the transmit signal has to be unipolar and real-valued due to the inherent linear intensity characteristics [3]. For transforming the bipolar signal into a real-valued unipolar format, in O-OFDM transmission, two methods are primarily used: DC-biased optical OFDM (DCO-OFDM), and asymmetrically clipped OFDM (ACO-OFDM) [4]. In both of the methods, a real-valued and bipolar time domain transmitting signal is acquired by expending half of the available bandwidth and by maintaining the property of Hermitian symmetry causing half of the spectrum loss [5]. In DCO-OFDM, introducing a DC bias after the modulation with a consequent zero clipping ensures the unipolarity of the transmitting signal [1]. On the other hand, ACO-OFDM arranges the data symbols on the odd-indexed subcarrier only and applies a clip to the even-indexed subcarriers to ensure the unipolarity of the signal [6]. Although ACO-OFDM resolves power inefficiency and signal distortion associated with DCO-OFDM [5], only one-fourth of the total subcarriers are allocated for data transmission, which leads to a substantial spectral loss [4]. Apart from the ACO-OFDM and DCO-OFDM, there are several other O-OFDM schemes developed in the literature, for example, the pulse-amplitude modulated discrete multitone (PAM-DMT), Flip-OFDM, unipolar (U)-OFDM systems etc [3], [5].

Orthogonal time frequency space (OTFS) is a recently proposed modulation technique in RF communication that has a promising prospect for high-mobility channels [7]. While traditional modulation schemes map the information symbol in either the time or frequency domain, in OTFS, the data symbols are mapped onto a two-dimensional (2D) delay-Doppler (DD) grid. This DD domain signal then undergoes OTFS modulation which enables the transmit signal to be resilient to both time and frequency dispersion [7].We note here that the conventional OTFS modulation is based on the Fourier transform (FT). Recently, OTFS has been deployed in OWC [2], [8]. Similar to RF systems, O-OTFS-based schemes provide performance improvements over other existing schemes, such as O-OFDM systems. However, existing research on O-OTFS relies on ACO and DCO techniques, which results in spectral inefficiency and higher peak-to-average power ratio (PAPR), as explained earlier.

In this context, we consider a modulation format incorporating wavelet transform (WT) in the conventional OTFS scheme to overcome its limitations [9]. WT offers a flexible resolution between time and frequency domains. This particular attribute allows WT-based systems more resilience towards Doppler shifts, leading to a much lower bit error rate (BER) in high-speed scenarios [10]. Leveraging this dual localization capability of wavelets, we can also improve spectral efficiency by eliminating the necessity for a cyclic prefix (CP). Additionally, by allowing multiresolution analysis, WT enables concentrating the signal energy in specific regions of the time-frequency plane, thus leading to a significant PAPR reduction [10].

979-8-3503-8577-9/24/$31.00 ©2024 IEEE

Authorized licensed use limited to: Khulna University. Downloaded on October 19,2026 at 07:19:22 UTC from IEEE Xplore. Restrictions apply.

Furthermore, WT is inherently flexible to significant signal length variations, which establishes its advantage in dynamic channel conditions. Motivated by these advantages of WT, we consider the integration of WT into the conventional OTFS system, leading to the modulation scheme termed as wavelet-aided OTFS (W-OTFS). Recently, a W-OTFS modulation-based communication scheme has emerged for reconfigurable intelligent surface (RIS)-aided high-mobility wireless channels [11]. As a further advance, we extend the application of W-OTFS to OWC systems, introducing a DC-biased W-OTFS (DCO W-OTFS) scheme. Our scheme eliminates the necessity for Hermitian symmetry, ensuring the preservation of the full spectral efficiency. By leveraging the advantages of WT, DCO W-OTFS achieves significantly reduced PAPR, resulting in lower power consumption without sacrificing bandwidth efficiency.

The key contributions of this study are summarized as follows:

1) The wavelet transform is incorporated into the OTFS system, thus a new scheme is introduced referred to as W-OTFS.
2) A DC-biased W-OTFS system is proposed for OWC that does not require Hermitian symmetry, thereby avoiding spectral loss.
3) The wavelet-based system is found to exhibit lower PAPR and BER. The implementation complexity of the wavelet-based system is also reduced.

The structure of the paper is as follows: Section II presents a brief introduction to the WT and discrete WT (DWT) matrix, while Section III provides a comprehensive overview of the proposed system architecture. Section IV presents the simulation results and their significance, and finally, Section V includes the paper's conclusion.

II. Wavelet Transform and Wavelet Matrices

Wavelets, characterized by some wave-like oscillations, have gained increasing popularity as a signal-processing tool in modern-day applications. WT is often preferred over FT owing to its simultaneous time and frequency resolution property. FT, which uses sinusoidal basis functions, results in excellent frequency resolution but it cannot precisely localize events in time. By contrast, WT utilizes wavelet basis functions which are simultaneously localized in both the domains. The simultaneous time and frequency domain localization property of wavelets enhances their effectiveness in capturing changes and transient features in signals.

Mathematically, wavelet transform can be represented as follows [9]:

$$WT\{g(t)\} = \int_{-\infty}^{\infty} g(t) \cdot \psi^* \left(\frac{t-\tau}{\nu} \right) dt. \tag{1}$$

Here, $g(t)$ represents the input signal, $\psi(t)$ denotes the mother wavelet, τ represents the time shift (delay), and ν represents the scale parameter (Doppler). The scale parameter ν can be varied to adjust the desired stretching or compression of the wavelet basis function. For comparing the contrasting approaches of FT and WT in signal analysis, let us consider a sharp impulse or a short burst of activity in a signal. By the fundamental principles of FT, it would spread this impulse across the entire frequency spectrum, which makes it impossible to retrieve its occurrence time exactly. On the other hand, WT can accurately detect the occurrence time, while providing information about its frequency content at the same time.

A. Orthogonal Wavelets: The Haar and Daubechies Wavelets

Orthogonal wavelets, such as the Haar and Daubechies wavelets, are among the most widely used wavelets due to their orthonormal basis functions, which offer simplifications in various mathematical operations. Daubechies wavelets employ finite-length scaling sequences (w_k) for the generation of the basis functions. A wavelet of order Z involves a sequence length of $k = 0, 1 \ldots\ldots (Z-1)$.

Using the scaling sequences (w_k), the scaling function $\phi(t)$ can be obtained using (2):

$$\phi(t) = \sum_{k=0}^{Z-1} w_k \phi(2t-k) \tag{2}$$

where the scaling coefficients w_k satisfy the criterion [9], [12]: $\sum_{k=0}^{Z-1} w_k = 2$.

To calculate scaling sequence coefficients w_k, we need to ensure that the scaling function $\phi(t)$ satisfies certain properties, such as orthogonality, admissibility property, and so on. In practice, various numerical and algebraic techniques are employed to calculate the values of w_k that meet these criteria. Fortunately, these coefficients for different versions of Daubechies wavelet, such as D2 to D20 (DZ) are available in literature [9], [13].

B. Wavelet Matrix

For our application, it is possible to construct a WT matrix ($\boldsymbol{W}$) utilizing w_k, such that $\boldsymbol{WS} = \mathrm{DWT}(\boldsymbol{S})$. The formation of the transformation matrix $\boldsymbol{W}_N$ for a specific transformation level N can be obtained by the cascade algorithm of [12]. When considering the transformation level $N = 8$, the matrix corresponding to D2 (or Haar) is shown below. Note that the Haar and D2 wavelets exhibit a similar configuration with two scaling coefficients, allowing for their interchangeable applications.

$$\boldsymbol{W}_8^{D2} = \begin{bmatrix} -w_1 & w_0 & 0 & 0 & 0 & 0 & 0 & 0 \\ 0 & 0 & -w_1 & w_0 & 0 & 0 & 0 & 0 \\ 0 & 0 & 0 & 0 & -w_1 & w_0 & 0 & 0 \\ 0 & 0 & 0 & 0 & 0 & 0 & -w_1 & w_0 \\ w_0 & w_1 & 0 & 0 & 0 & 0 & 0 & 0 \\ 0 & 0 & w_0 & w_1 & 0 & 0 & 0 & 0 \\ 0 & 0 & 0 & 0 & w_0 & w_1 & 0 & 0 \\ 0 & 0 & 0 & 0 & 0 & 0 & w_0 & w_1 \end{bmatrix}.$$

For an N-level transformation, the transformation matrix is of size $N \times N$. This requires appending $(N-Z)$ zeros to each row of the matrix after incorporating the Z number

Authorized licensed use limited to: Khulna University. Downloaded on October 19,2026 at 07:19:22 UTC from IEEE Xplore. Restrictions apply.

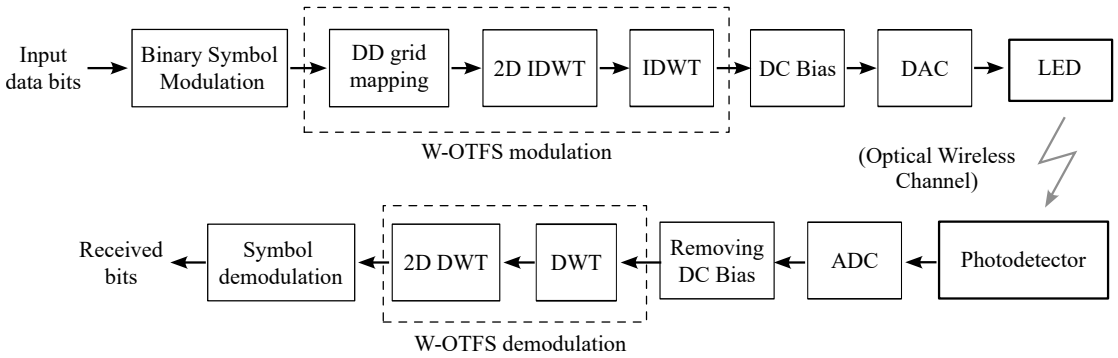


Fig. 1: Block diagram of the proposed DCO W-OTFS scheme.

of scaling coefficients (w_k) for the specific wavelet DZ. In the construction of the wavelet matrix $\boldsymbol{W}$, the arrangement of scaling sequence coefficients w_k involves organizing them with consecutive 2-shifts for the last four rows. For the elements in the first four rows, the process includes flipping the scaling sequence coefficients w_k first, followed by consecutive 2-shifts, and alternating in sign [12].

As a further note, the $N-$point DFT matrix $\boldsymbol{F}_N$ contains no entities with a value of 0. On the other hand, when examining the matrix $\boldsymbol{W}$, the presence of 0-valued entities increases as the Daubechies order decreases. This observation offers a clear insight that with lower order Daubechies wavelets, especially with D2 (Haar) or D4 wavelets, the multiplication complexity in transformation operation is consistently lower than that of DFT. Specifically, when it comes to the multiplication complexity of the DFT matrix, it is of the order $O\left(N^2\right)$. By contrast, for the Haar and D4 matrices, the complexity reduces significantly to $O\left(2N\right)$ and $O\left(4N\right)$, respectively.

III. The Proposed System Architecture

Fig. 1 depicts the proposed DCO W-OTFS system model. As illustrated, a binary modulation technique is employed, ensuring that the transmitting symbols are real-valued. The frequency domain symbols are then converted to a time domain signal using W-OTFS modulation, which introduces no complex terms in the signal. Consequently, the transmitting time-domain signal remains entirely real. Following this, the bipolar signal is shifted into the positive domain with the aid of a DC bias. The applied DC bias is first removed from the received electrical domain signal at the receiver side, and the resulting signal then undergoes W-OTFS demodulation. The model is detailed in the subsequent sections.

A. Transmitter Processing

As depicted in Fig. 1, the data bits are first mapped to symbols using the binary phase shift keying (BPSK) or quadrature PSK (QPSK) constellation. The symbols are subsequently placed on a two-dimensional data grid ($\boldsymbol{X}$) known as the DD grid. Following this, symbols in the DD grid undergo modulation through the W-OTFS. As evident from Section II-B, the wavelet transform matrix $\boldsymbol{W}$ is entirely real. By employing binary modulation techniques for symbol

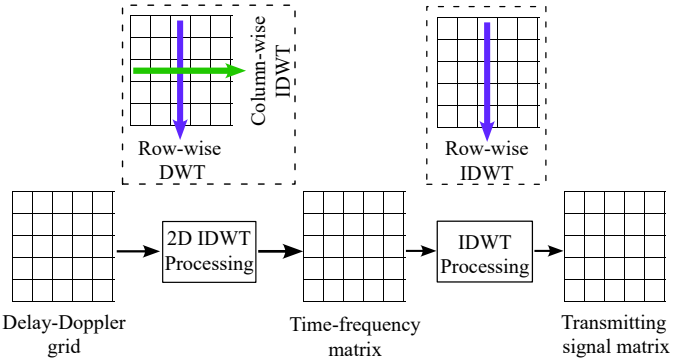


Fig. 2: W-OTFS modulation scheme for multicarrier OWC

modulation, we can achieve a completely real multicarrier-modulated transmitting signal using W-OTFS. This approach eliminates the need for implementing the Hermitian symmetry, thus preventing spectral efficiency loss.

The proposed W-OTFS modulation involves a two-step procedure illustrated in Fig. 2. Initially, the DD symbols undergo conversion to the time-frequency (TF) domain through a 2D inverse discrete wavelet transform (IDWT) operation. The 2D-IDWT is executed by applying M-level DWT across the columns and N-level IDWT across the rows of the DD frame. The resulting TF domain signal matrix then undergoes IDWT across its columns to generate a time-domain (TD) signal. This process ensures the preservation of orthogonality and separability among subcarriers in the resulting time domain signal. If we consider the adoption of a rectangular pulse-shaping waveform, the expression for the W-OTFS modulated signal is as follows:

$$\boldsymbol{S} = \boldsymbol{W}_M^T \left(\boldsymbol{W}_M \boldsymbol{X} \boldsymbol{W}_N^T \right), \tag{3}$$

where M and N represent the respective counts of rows and columns within the DD grid. $\boldsymbol{W}_M$ and $\boldsymbol{W}_M^T$ denotes the M-level DWT and IDWT matrices, respectively. It is worth noting that the orthogonality property of the used wavelets allows us to obtain the IDWT matrix by transposing the DWT matrix [14].

The matrix $\boldsymbol{S}$ representing the time-domain (TD) signal

Authorized licensed use limited to: Khulna University. Downloaded on October 19,2026 at 07:19:22 UTC from IEEE Xplore. Restrictions apply.

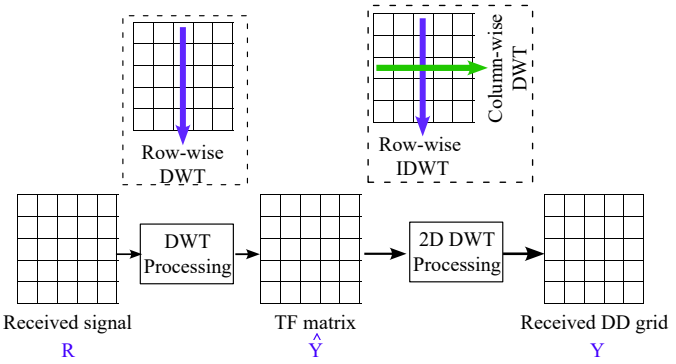


Fig. 3: W-OTFS demodulation scheme for multicarrier OWC

($\boldsymbol{S} \in \mathbb{C}^{M\times N}$) is transformed into a vectorized TD signal $\hat{\boldsymbol{s}} \in \mathbb{C}^{MN\times 1}$, *i.e.* $\hat{\boldsymbol{s}} = \text{vec}(\boldsymbol{S})$, where the notation vec $(\bullet)$ denotes the operation of stacking the columns of the matrix '$\bullet$' into a vector. The signal $\hat{\boldsymbol{s}}$ is a real bipolar signal. However, the optical spectrum can not deal with negative signals. To address this, a suitable DC bias, denoted as b, is introduced to the time-domain signal $\hat{\boldsymbol{s}}$ to push it into the positive domain. Consequently, the expression for the transmitting signal is as follows:

$$\boldsymbol{s} = \hat{\boldsymbol{s}} + b. \tag{4}$$

The selection of the bias b requires careful consideration. A large bias voltage leads to a higher PAPR, while a minimal bias voltage retains a significant portion of the signal in the negative domain. Usually, a moderate bias voltage is utilized, and any negative peaks that persist after applying the bias voltage are truncated at zero. The resultant time-domain electrical signal undergoes digital-to-analog conversion and is subsequently subjected to optical modulation. In this study, an ideal optical modulator is considered, wherein the intensity of the resulting optical signal $\boldsymbol{s}_o$ is directly proportional to the input electrical current [4].

At this point, we try to investigate the complexity of W-OTFS modulation and compare it with that of OTFS. Considering $\boldsymbol{S}_{\text{W-OTFS}} = \boldsymbol{W}_M^T \left(\boldsymbol{W}_M \boldsymbol{X} \boldsymbol{W}_N^T\right)$ and $\boldsymbol{S}_{\text{OTFS}} = \boldsymbol{F}_M^H \left(\boldsymbol{W}_M \boldsymbol{X} \boldsymbol{F}_N^H\right)$, the asymptotic complexity for W-OTFS and OTFS modulations are: $C_{\text{W-OTFS}} = \mathcal{O}(N+M)$ and $C_{\text{OTFS}} = \mathcal{O}(N \log_2 N + M \log_2 M)$ respectively. This shows that the complexity of W-OTFS modulation is reduced compared to conventional OTFS. It is worth mentioning that the asymptotic complexities for an $N-$point FFT and $N-$level DWT algorithms are given by $O(N \log_2 N)$ and $O(N)$, respectively.

B. Behaviour of Optical Wireless Channels

The transmitting optical signal $\boldsymbol{s}_o$ is sent through an optical wireless channel characterized by the impulse response $h_o(t)$. The received optical signal $\hat{x}(t) = h_o(t) \otimes s_o(t)$ is processed by a direct detection receiver (IM/DD system [6]) converting optical intensity into an electrical signal. Here, the symbol $\otimes$ denotes the convolution operation. Let us consider $h(t)$ as the combined impulse response governing the conversion from optical to electrical signals. Hence, in a noise-free receiver, the received electrical signal is represented as $h(t) \otimes \hat{x}(t)$ [6].

Typically, optical wireless channels can function in either directed or non-directed modes. In the directed mode, line-of-sight (LOS) paths are prominent. A simple additive white Gaussian noise (AWGN) channel model is suitable to model this link. However, this AWGN assumption does not hold for non-directed or diffused optical wireless channels. We consider the optical wireless channel as a linear baseband channel [5], [6]. Assuming $v(t)$ as AWGN noise, the received electrical signal can be modeled as:

$$r(t) = h(t) \otimes \hat{x}(t) + v(t). \tag{5}$$

C. Receicer Processing

At the receiver, an ideal photodiode, wherein the resulting electrical current is directly proportional to the intensity of the received optical signal, is employed to convert the received optical signal into the electrical signal. From the received electrical signal vector $\boldsymbol{r}$, we first exclude the DC bias added in the transmitter, which implies:

$$\hat{\boldsymbol{r}} = \boldsymbol{r} - b. \tag{6}$$

The resulting electrical signal undergoes W-OTFS demodulation, followed by the symbol-to-bits demapping. The demodulation process of W-OTFS also involves two steps. At first, we obtain the TF domain received signal matrix, $\hat{\boldsymbol{Y}} \in \mathbb{C}^{M\times N}$ through a DWT applied across the column of the received TD signal matrix, $\boldsymbol{R} = \text{vec}^{-1}(\hat{\boldsymbol{r}})$. The received TF domain signal matrix, $\hat{\boldsymbol{Y}}$ is transformed into the received DD symbol grid $\boldsymbol{Y}$ using a 2D-DWT. The 2D-DWT is executed by applying M-level IDWT across the columns and N-level DWT across the rows of TF domain signal matrix $\hat{\boldsymbol{Y}}$, as shown in Fig 3. Assuming that rectangular pulse shaping is used, the W-OTFS demodulated received symbol $\boldsymbol{Y}$ can be expressed as:

$$\boldsymbol{Y} = \boldsymbol{W}_M^T \left(\boldsymbol{W}_M \boldsymbol{R}\right) \boldsymbol{W}_N. \tag{7}$$

The matrix representing received symbols in the DD domain, denoted as $\boldsymbol{Y} \in \mathbb{C}^{M\times N}$, is transformed into a vectorized DD symbol sequence $\boldsymbol{y} \in \mathbb{C}^{MN\times 1}$, which then undergoes BPSK demodulation, yielding the received bits.

The complexity of demodulation in W-OTFS and OTFS is contingent upon the complexity of DWT/IDWT and DFT/IDFT, respectively. Following the same reasoning outlined in Section III-A, the demodulation complexity of W-OTFS is lesser to that of OTFS.

IV. Results and Discussion

Here, we investigate the performance of the proposed W-OTFS system for optical wireless communication. We set the number of subcarriers (M) of the DD grid to 8 and the symbols per subcarrier (N) to 8 as well. Consequently, an 8×8 DD grid is generated. We chose $b = 4$, and negative peak clipping was not used. We used a frame size of $10,000$. The error

Authorized licensed use limited to: Khulna University. Downloaded on October 19,2026 at 07:19:22 UTC from IEEE Xplore. Restrictions apply.

TABLE I: Comparison of popular multicarrier schemes for OWC

	CP length	Diversity gain	PAPR	BER	Hermitian symmetry
DCO OFDM	High	No	High	High	Used
ACO OFDM	High	No	High	High	Used
DCO OTFS	Reduced [7]	Moderate [2]	Moderate	Moderate	Used
ACO OTFS	Reduced [7]	Moderate [2]	Moderate	Moderate	Used
Proposed DCO W-OTFS	No CP	High [11]	Low	Low	Not used

performance of the system and the signal's PAPR are shown in Section IV-A and Section IV-B, respectively.

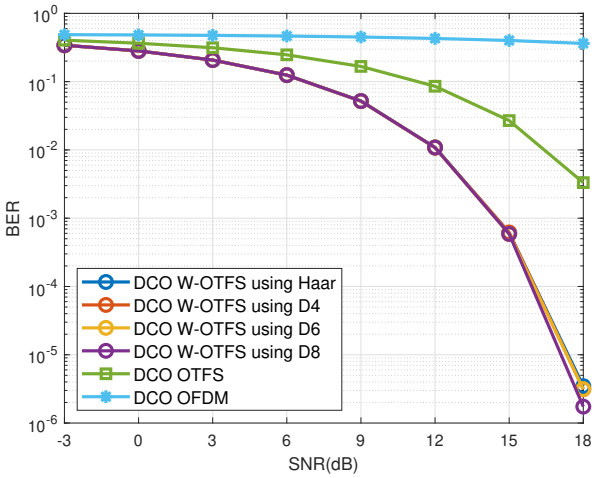


Fig. 4: BER performance of DCO W-OTFS

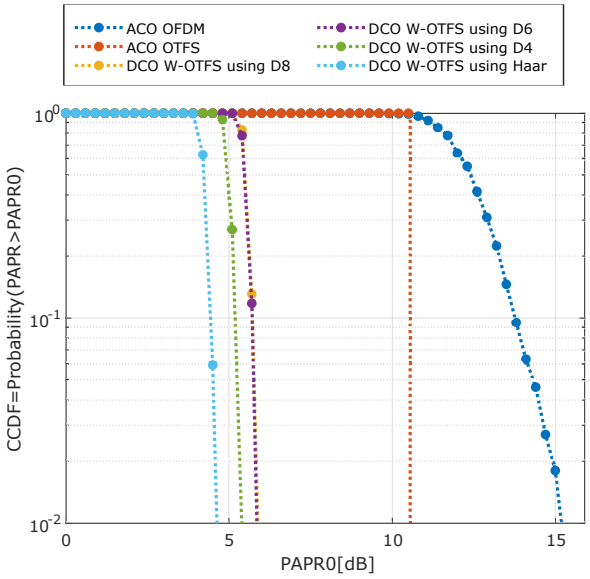


Fig. 5: PAPR performance of DCO W-OTFS

A. Error Performance

Fig. 4 illustrates the BER of the W-OTFS-based optical wireless system. It is evident that the DCO W-OTFS system consistently achieves a lower BER than both DCO OFDM and DCO OTFS systems. Several previous studies have reported that O-OTFS exhibits better BER performance than O-OFDM [2], [8]. By leveraging the double localization property of wavelets (see Section II), the wavelet-based systems reduce intersymbol interference (ISI) more effectively, resulting in further improved BER. Fig. 4 also demonstrates the impact of various wavelet versions on the system performance of the DCO W-OTFS. As evident, the BER is consistent with all the employed wavelets. However, as highlighted in Section II-B, the Haar wavelet produces the most sparse transformation matrix, leading to a less complex transformation operation and implying low-complexity modulation and demodulation. Therefore, the Haar wavelet emerges as the preferred choice for the DCO W-OTFS modulation.

B. Signal PAPR: Comparative Analysis

DCO systems usually suffer from a high PAPR [4]. However, the wavelets can concentrate signal energy in specific time-frequency regions [10]. As a result, the high PAPR problem is resolved. As illustrated in Fig. 5, where we use $N = 12$ and $M = 256$, the DCO W-OTFS signal has a lower PAPR than the ACO-OTFS signal. The performance is further improved when compared to the ACO-OFDM system. For instance, using the Haar-modulated DCO W-OTFS system, we achieve a PAPR reduction of approximately 6 dB and 10 dB compared to ACO-OTFS and ACO-OFDM, respectively, at a complementary cumulative distribution function (CCDF) of 10^{-2}. Similar reductions are observed with other Daubechies wavelets, with lower-order wavelets demonstrating improved PAPR performance. Specifically, the D6 and D8-based systems show a PAPR reduction of approximately 5 dB and 9 dB compared to ACO-OTFS and ACO-OFDM, respectively, at CCDF=10^{-2}. For the D4-modulated DCO W-OTFS system, we observe a PAPR reduction of approximately 5.5 dB and 9.5 dB compared to ACO-OTFS and ACO-OFDM, respectively, at the same CCDF level.

V. Conclusion

We have proposed a W-OTFS-based DCO system for OWC in this paper. We investigate the Haar and Daubechies wavelets and it is found that lower-order wavelets offer sparse transformation matrix and thus exhibit decreased computational complexity. The well-known PAPR challenge of the DCO-based systems is compensated with the aid of wavelet-based

Authorized licensed use limited to: Khulna University. Downloaded on October 19,2026 at 07:19:22 UTC from IEEE Xplore. Restrictions apply.

modulation by leveraging its energy concentration property. Accordingly, lower-order wavelets, exemplified by the Haar wavelet, demonstrate a significant PAPR reduction of approximately 6 dB and 10 dB compared to the ACO-based OTFS and OFDM systems, respectively (refer to Section IV-B for details). Moreover, the entirely real wavelet transform matrix in conjunction with a second-order constellation enables a fully real multicarrier-modulated W-OTFS transmit signal, which disposes of the requirement of implementing Hermitian symmetry and thus retains the spectral efficiency. These findings are succinctly presented in Table I to facilitate a comprehensive understanding of our proposed W-OTFS-based DCO scheme. In conclusion, our proposed W-OTFS-based DCO scheme, leveraging the advantages of wavelet-based modulation and lower-order wavelets, offers a promising solution for addressing the spectral inefficiency, and PAPR challenges in multicarrier OWC, plus, it offers reduced computational complexity and improved error performance.

REFERENCES

[1] J. Armstrong, "OFDM for optical communications," *J. Lightw. Technol.*, vol. 27, no. 3, pp. 189–204, 2009.

[2] C. Xu, X. Zhang, P. Petropoulos, S. Sugiura, R. G. Maunder, L.-L. Yang, Z. Wang, J. Yuan, H. Haas, and L. Hanzo, "Optical OTFS is capable of improving the bandwidth-, power-and energy-efficiency of Optical OFDM," *IEEE Trans. Commun.*, 2023.

[3] X. Zhang, Z. Babar, P. Petropoulos, H. Haas, and L. Hanzo, "The evolution of optical OFDM," *IEEE Commun. Surveys Tuts.*, vol. 23, no. 3, pp. 1430–1457, 2021.

[4] S. D. Dissanayake and J. Armstrong, "Comparison of ACO-OFDM, DCO-OFDM and ADO-OFDM in IM/DD systems," *J. Lightw. Technol.*, vol. 31, no. 7, pp. 1063–1072, 2013.

[5] N. Fernando, Y. Hong, and E. Viterbo, "Flip-OFDM for unipolar communication systems," *IEEE Trans. Commun.*, vol. 60, no. 12, pp. 3726–3733, 2012.

[6] X. Li, R. Mardling, and J. Armstrong, "Channel capacity of IM/DD optical communication systems and of ACO-OFDM," in *2007 IEEE International Conference on Communications*, 2007, pp. 2128–2133.

[7] P. Raviteja, Y. Hong, E. Viterbo, and E. Biglieri, "Practical pulse-shaping waveforms for reduced-cyclic-prefix OTFS," *IEEE Trans. Veh. Technol.*, vol. 68, no. 1, pp. 957–961, 2018.

[8] D. Zheng, H. Zhang, and J. Song, "DCO-OTFS-based full-duplex relay-assisted visible light communications," *Optics Express*, vol. 29, no. 25, pp. 41 323–41 332, 2021.

[9] I. Daubechies, *Ten lectures on wavelets*. SIAM, Philadelphia, PA, 1992.

[10] M. Chafii, Y. J. Harbi, and A. G. Burr, "Wavelet-OFDM vs. OFDM: Performance comparison," in *2016 23rd International conference on telecommunications (ICT)*. IEEE, 2016, pp. 1–5.

[11] M. H. Abid, I. A. Talin, and M. I. Kadir, "Wavelet-aided OTFS for RIS-assisted high-mobility wireless channels," *IEEE Wireless Commun. Lett.*, 2024.

[12] I. Daubechies and J. C. Lagarias, "Two-scale difference equations II. local regularity, infinite products of matrices and fractals," *SIAM Journal on Mathematical Analysis*, vol. 23, no. 4, pp. 1031–1079, 1992.

[13] J. R. Williams and K. Amaratunga, "Introduction to wavelets in engineering," *International journal for numerical methods in engineering*, vol. 37, no. 14, pp. 2365–2388, 1994.

[14] J. Gilles, "Empirical wavelet transform," *IEEE Trans. Signal Process.*, vol. 61, no. 16, pp. 3999–4010, 2013.

Authorized licensed use limited to: Khulna University. Downloaded on October 19,2026 at 07:19:22 UTC from IEEE Xplore. Restrictions apply.